NASA TM-84300

NASA Technical Memorandum 84300

A Nonintrusive Laser Interferometer Method for Measurement of Skin Friction

Daryl J. Monson

October 1982

NASA
National Aeronautics and
Space Administration

NASA Technical Memorandum 84300

A Nonintrusive Laser Interferometer Method for Measurement of Skin Friction

Daryl J. Monson, Ames Research Center, Moffett Field, California

NASA
National Aeronautics and
Space Administration

Ames Research Center
Moffett Field, California 94035

Abstract

A method is described for monitoring the changing thickness of a thin oil film subject to an aerodynamic shear stress using two focused laser beams. The measurement is then simply analyzed in terms of the surface skin friction of the flow. The analysis includes the effects of arbitrarily large pressure and skin-friction gradients, gravity, and time-varying oil temperature. It may also be applied to three-dimensional flows with unknown direction. Applications are presented for a variety of flows including two-dimensional flows, three-dimensional swirling flows, separated flows, supersonic high Reynolds number flows, and delta-wing vortical flows.

List of Symbols

A = dT/dt [see Eq. (9)]

C_f = local skin-friction coefficient, τ/q

dp/dx = external flow pressure gradient

g = gravitational acceleration

H = step height

I = incidence angle for interferometer flat

i = laser beam incidence angle measured from the normal to a surface

M = Mach number

N = fringe number

n = coordinate perpendicular to oil-flow direction (see Fig. 4).

n_g = interferometer flat index of refraction

n_o = oil index of refraction

q = free-stream dynamic pressure

R = Reynolds number; also, refraction angle for interferometer flat

r = laser beam refraction angle within oil measured from the normal to a surface

S = oil-viscosity/temperature-slope [see Eq. (11)]

s = coordinate along oil-flow direction (see Fig. 4); also, delta wing semispan

T = temperature; also, interferometer flat thickness

t = time

V_∞ = tunnel free-stream speed

w_s = transverse speed on surface of rotating cylinder

x = coordinate parallel to line joining beams (see Fig. 4); also, distance downstream from step

Y_o = tunnel height

y = oil thickness; also, delta wing semispan distance

z = coordinate perpendicular to line joining beams (see Fig. 4)

α = tunnel-wall deflection angle; also, delta-wing angle of attack

γ = local oil-flow angle with respect to the x coordinate (see Fig. 4)

ΔN = incremental change in fringe number

Δt = incremental change in time

Δx = beam spacing

δ = boundary-layer thickness

ε = pressure gradient and gravity-correction parameter [see Eq. (8)]

θ = surface inclination from horizontal

λ = laser wavelength

ν = oil kinematic viscosity

ρ = oil density

τ = local skin friction

Superscripts

$( )'$ = corrected or "effective" value

$\overline{( )}$ = average value

Subscripts

L = model length

x,z = directions as shown in Fig. 4

$1,2,3,4$ = refer to positions in Figs. 1 and 4, or to times in Fig. 3

∞ = free-stream conditions

θ = momentum thickness

1. Introduction

The importance of skin-friction data in aerodynamic testing has stimulated the development of a wide variety of skin friction methods for the measurement of data in both two- and three-dimensional flows. Winter (1977) describes the principal methods for two-dimensional flows. These methods include the free-floating element balance, the analysis of mean-velocity data with the Clauser chart included, the Preston tube, and surface thin-film heat-transfer gauges. Measuring skin friction in three-dimensional flows is more difficult, and fewer methods have been developed. For such flows, McAllister, Pierce, and Tennant (1982) use a free-floating element balance, Higuchi and Peake (1978) use a bidirectional buried-wire gauge, and Higuchi and Rubesin (1981) use a bidirectional surface-fence gauge.

Although the above methods have been widely used, they all are seriously limited in one or more respects. For example, whereas the free-floating element balance measures skin friction directly, it is delicate, expensive, difficult to fabricate and calibrate, and subject to unknown element misalignment and pressure-gradient errors. The other methods are based on near-wall flow similarity and, thus, measure skin friction only indirectly. Consequently, the applicability of these methods is limited. They also require either permanent installation in a surface or are intrusive to the flow. Clearly, new and reliable methods for measuring skin friction in both two- and three-dimensional flows are desirable.

One new approach is the oil-viscosity balance method first described by Tanner (1977), in which he used a laser interferometer to measure the thickness of a thin oil film flowing on a surface subject to shear stress. This approach has the important advantage of being a direct method similar to the floating-element balance and consequently does not require calibration in a known flow. It can also be used in either a two- or a three-dimensional steady flow. Additionally, this method is inexpensive, simple to use, potentially very accurate, easy to relocate at various test points, and nonintrusive.

The development of the method has progressed through several steps. Tanner (1977) verified the first version of the method in a low-speed, two-dimensional, flat-plate flow. Monson and Higuchi (1981) described a more practical, two-beam instrument that allows easy test point relocation and eliminates the need to visually locate the oil leading-edge position. The theory for the method was also extended, thus eliminating the need to measure total oil flow time. This method was verified in a low-speed simple flow. Monson, Driver, and Szodruch (1981) further extended the theory for the method to account for the change in oil temperature and to allow application to three-dimensional flows. The preceding method was verified in separated flows, high-Reynolds-number supersonic flows, and complex flows on a delta wing. Finally, Monson (1983) verified the accuracy of the three-dimensional flow method with measurements in a swirling three-dimensional boundary-layer flow.

This paper reviews the laser interferometer method for measuring skin friction and presents examples of its application to a variety of flows.

2. The Laser Interferometer Technique

2.1 Principle

Figure 1 illustrates the principle of the two-beam laser-interferometer skin-friction method as described by Monson and Higuchi (1981). Two laser beams with known spacing are focused on a surface such that the line between them is parallel to the desired measurement direction. This direction is usually aligned with the known surface flow direction. (Special requirements on the oil-line geometry are discussed in Section 2.3 for cases in which the measurement and flow directions differ.) A line of oil is applied ahead of the front beam, the flow is started, and the oil flows downstream past the two beams. The laser beams measure the time rate of change of the oil film's slope by monitoring the time-dependent optical interference as discussed in Section 2.2. This information, in turn, is used to compute the

average skin friction during the measurement period using the oil-flow theory and data-reduction equations discussed in Section 2.3.

2.2 Instrument

A schematic of the two-beam instrument developed by Monson and Higuchi (1981) is shown in Fig. 2. The linearly polarized output from a He-Ne laser is expanded and passed through a neutral-density filter to reduce its power to a level that avoids the effects of local oil heating [see discussion by Tanner (1977)]. The single beam is then split into two parallel beams of known spacing with an angled interferometer flat. In the notation of Fig. 1, the beam spacing, Δx, is determined by the properties of the interferometer flat as

$$\Delta x = 2T \cos(I) \tan(R) \quad , \tag{1}$$

where

$$\tan(R) = \tan [\arcsin(\sin(I)/n_g)] \quad .$$

[For example, Monson and Higuchi (1981) used a fused silica flat 6.4 mm thick with a 45° incidence angle to achieve a beam spacing of 5 mm.] One beam passes through a half-wave retardation plate to rotate its polarization 90°, and then both beams are focused on a polished model surface or wall containing an oil film. The beams reflect from both the surface and the oil, causing optical interference. The two beams of crossed polarization are then separated with a polarization beam splitter and focused on separate photodiodes. Additional polarizers and filters at the photodiodes provide further signal isolation and background noise reduction. The photodiode signals may then be recorded on a two-channel chart recorder or another appropriate device. As the oil thickness changes, the light intensities in each beam are modulated by alternating constructive and destructive interference between the oil and surface reflections. A typical recorded fringe record is shown in Fig. 3. The transmitting and receiving components are mounted on separate tripods to allow versatile test positioning of the laser beams.

A NONINTRUSIVE LASER INTERFEROMETER METHOD FOR MEASUREMENT OF SKIN FRICTION

Daryl J. Monson*

NASA Ames Research Center, M/S 230-3,
Moffett Field, California 94035, U.S.A.

Suggested running head:

Laser Skin-Friction Method

*Research Scientist, Physical Sciences Branch

The only constraint on the geometry pertains to the laser-beam incidence angle. The two-beam instrument cannot be used if wind-tunnel geometries require angles in the range between 30° and 70°. There, the angles are too near the oil Brewster angle of 54°, where the oil reflects the p-polarization poorly. One method of avoiding this problem is to increase the incidence angle to a value beyond 70°. This grazing-incidence method is described in more detail by Monson et al. (1981). Another solution is to use only an s-polarized beam and to apply the single-beam method described in Section 2.3.

2.3 Theory

Tanner and Blows (1976) showed that the skin friction can be related to the slope of an oil film flowing from the action of shear stress according to

$$\tau = \frac{\rho \nu x}{yt} = \frac{\rho \nu}{t \, \partial y/\partial x} \quad , \tag{2}$$

where the notation is from Fig. 1. The quantities on the right-hand side can all be measured. Oil density and viscosity are determined in advance as a function of temperature. The remaining quantities may be measured with the two-beam laser interferometer method described in Section 2.1. The data-reduction equations derived by Monson et al. (1981) are summarized here in their generalized version. Simpler versions pertinent to special flows will also be presented in this section.

The generalized data-reduction equations are derived with reference to Fig. 4 for flows with unknown direction. As shown, the focused beams from a two-beam laser transmitter impinge on the oil at points (1) and (2) located along a line in the desired measurement direction, defined here as the x axis. A straight line of oil is assumed to be applied along the z axis upstream of beam (1) orthogonal to the x axis. Because of shear stress, the oil then flows along streamlines aligned at an unknown angle, γ, which defines the rotated coordinate system (s,n) where s is aligned with the local flow direction. Oil streamline curvature in this small region is neglected.

Arbitrary pressure and skin-friction gradients, gravity forces, and a changing oil temperature are taken into account.

Using the conditions above and the notation of Figs. (1), (3), and (4), the x component of skin friction at point (3) corrected for pressure and gravity gradients is

$$\tau'_{3x} = \tau_{3x}/(1 - \varepsilon_x) \quad . \tag{3}$$

Here, τ_{3x} is the uncorrected skin friction given by

$$\tau_{3x} = \frac{2\, n_o\, \rho \nu_1\, \cos(r)}{\lambda} \cdot \frac{\Delta x}{(N'_1\, t'_1 - N'_2\, t'_2)} \tag{4}$$

with

$$\left.\begin{aligned} N'_1 &= -\Delta N_1 \frac{\frac{\Delta N_2}{\Delta N_1}\left(\frac{\Delta t'_2}{\Delta t'_1} - 1\right)}{\left(\frac{\Delta t'_2}{\Delta t'_1} - \frac{\Delta N_2}{\Delta N_1}\right)} \quad , \\ t'_1 &= -\Delta t'_1\left(\frac{N'_1}{\Delta t'_1} + 1\right) \quad , \\ t'_2 &= (t'_1 + \Delta t'_4) \quad , \\ N'_2 &= -\Delta N_3\left(\frac{t'_2}{\Delta t'_3} + 1\right) \quad , \end{aligned}\right\} \tag{5}$$

$$\left.\begin{aligned} \Delta t'_i &= \frac{1}{SA}\,[\exp(SA\Delta t_i) - 1] \\ &\cong \Delta t_i\left(1 + \frac{1}{2}\, SA\Delta t_i\right) \end{aligned}\right\} i = 1,2,4$$

$$\left.\begin{aligned} \Delta t'_3 &= \frac{\exp(SA\Delta t_4)}{SA}\,[\exp(SA\Delta t_3) - 1] \\ &\cong (1 + SA\Delta t_4)\,\Delta t_3\left(1 + \frac{1}{2} SA\Delta t_3\right) \quad , \end{aligned}\right\} \tag{6}$$

$$\cos(r) = \cos\left[\arcsin\left(\frac{\sin(i)}{n_o}\right)\right] \quad , \tag{7}$$

and

$$\varepsilon_x \cong \frac{\lambda \overline{N_1'}}{2n_o \tau_{3x} \cos(r)} \left[\frac{d\rho}{dx} - \left(\rho g \sin(\theta) \right)_x \right] \quad . \tag{8}$$

In the above equations, A is determined by a direct wall-temperature measurement as

$$A = (T_2 - T_1)/\Delta t_2 \quad , \tag{9}$$

so that the temperature variation during a measurement may be expressed as

$$T(t) \cong T_1 + A(t - t_1') \quad . \tag{10}$$

The parameter, S, is a predetermined oil constant in the oil viscosity-temperature equation

$$\nu(t) = \nu_1 \exp\left[-S(T(t) - T_1)\right] \quad . \tag{11}$$

In Eq. (8), the term $(\rho g \sin(\theta))_x$ is the gravity component in the x direction, and $\overline{N_1'}$ is a time averaged value for fringe number at point (1). Monson (1983) finds that a value

$$\overline{N_1'} \cong (N_1' + \Delta N_2/2) \tag{12}$$

is a reasonable choice based on measurements where the skin friction was known and a gravity force was present. In making skin-friction measurements in the presence of gravity or pressure gradients, accuracy is enhanced if care is taken to keep the value of the correction parameter, ε_x, less than a few percent of unity. This parameter can be controlled by taking data only after the oil film has thinned to the extent that the value of $\overline{N_1'}$ in Eq. (8) becomes sufficiently small.

Note that the skin-friction gradients do not appear explicitly in the above set of equations. However, Monson (1983) shows that the effect of the gradients can be made negligibly small to first order even for large gradients when the analysis is applied at point (3) between points (1) and (2) as shown in Fig. 4.

Although the above equations are derived for the x component of skin friction, the analysis is applicable for any direction. The only requirements are that the applied line of oil is straight and perpendicular to the measurement direction if it

differs from the local flow direction, and that the gradients in Eq. (8) are taken along the measurement direction. For example, by rotating the laser beam and oil orientations 90° in Fig. 4, the orthogonal skin-friction component, τ'_{3z}, is measured. By measuring two skin-friction components, the total skin-friction magnitude and flow direction at that point are obtained in a flow with unknown direction.

The general set of data-reduction equations presented here can be simplified for certain special flows. First, for constant temperature, A in Eq. (6) is zero and the corrected and measured time increments are equal. Second, ε_x is zero when no pressure or gravity gradients are present. The corrected and uncorrected skin friction in Eq. (3) are then equal. Third, for small skin-friction gradients, the requirement on positioning the laser beams at the measurement point (3) can be relaxed. Fourth, if the local flow direction is known and is equal to the measurement direction, the applied oil line need be neither straight nor perpendicular to the measurement direction. Finally, in some flows a single-beam method may be more convenient. This is done by using the front beam to locate the oil leading edge visually [see Tanner (1977)]. Then the product, $N'_2 t'_2$, in Eq. (4) is zero, and the known beam spacing, Δx, simply becomes the distance from the oil leading edge to the downstream beam position at point (1).

3.0 Experimental Verifications

3.1 Axisymmetric Two-Dimensional Boundary-Layer Flow

The initial verification experiments for the two-beam laser interferometer method were performed by Monson and Higuchi (1981) and later repeated by Monson (1983) in a simple two-dimensional boundary-layer flow with no gradients. The test facility was a low-speed wind tunnel sketched in Fig. 5. The tunnel has a cylinder mounted along its centerline on which the skin friction was measured. (A section of the cylinder can be rotated to produce a swirling boundary layer, but the cylinder was stationary for these tests.) Freestream flow speeds up to 50 m/s are possible.

Large plexiglass side windows allow laser beam access in and out of the tunnel. The oil temperature was measured with a thermocouple in the cylinder.

Monson and Higuchi (1981) measured skin friction on the cylinder using the laser interferometer method, a Preston tube, and a "law-of-the-wall" method. They found excellent agreement between all methods and with the predictions of a turbulent boundary-layer code. The only problem encountered was from occasional dust in the oil which caused erratic signals.

Monson (1983) later repeated the measurements on the cylinder using a dust filter at the tunnel inlet. A large number of measurements were made at each location so that an uncertainty analysis on the accuracy of the method could be performed. Those results are presented in Fig. 6 along with measurements using a surface-fence gauge and a theoretical prediction. As before, agreement between the two methods and with theory is excellent.

The error bars on the mean laser interferometer data represent confidence limits of 95%. These limits are assessed using the RMS uncertainty analysis of Kline and McClintock (1953). The analysis includes the uncertainty in computed skin friction which arises from the estimated fixed uncertainty in the data-reduction variables. It also includes twice the standard deviation due to random variations within the set of repeated measurements at each position. Based on these estimates, the accuracy of the laser interferometer method is within ±5%, at least for this simple flow. This accuracy compares with an estimated ±10% uncertainty in the calibration of the surface-fence gauge.

3.2 Axisymmetric Swirling Three-Dimensional Boundary-Layer Flow

Verification experiments for the three-dimensional flow version of the laser interferometer method were performed by Monson (1983) in the same low-speed wind tunnel described in Section 3.1. These experiments incorporated the rotating section of the center cylinder to produce a spinning boundary layer. The swirling boundary

layer is convected to a downstream stationary segment where it becomes three-dimensional as it begins turning through 90° and relaxing toward a stream parallel to the tunnel axis. Skin-friction measurements in the axial and transverse directions were made at several axial positions on the downstream stationary segment. The precision required in applying the oil line in three-dimensional flows was achieved by applying oil to the edge of a contoured plastic card, and then, guided by alignment marks, touching the card edge to the cylinder. The axial measurements and some of the transverse measurements were performed with the two-beam method. However, when the flow angle was shallow, the transverse measurements were made with the single-beam method to shorten the distance between the measuring point and the initial oil position and thus reduce problems with surface waves.

The two skin-friction components, C_{fx} and C_{fz}, measured at several axial positions, are compared in Fig. 7 with measurements using a bidirectional surface-fence gauge and with a theoretical calculation including cylinder spin. Excellent agreement between the two methods and with theory is observed for the axial components. The error bars on the laser interferometer data show comparable accuracy to the zero-spin data discussed in Section 3.1. Except for the last downstream position, excellent agreement between the two methods is also found for the transverse components. Agreement with theory is not as good as in the transverse direction, but Higuchi and Rubesin (1981) attribute this to limitations in the turbulence model.

The poor agreement between the experimental methods for the transverse direction at the last downstream position can be attributed to errors arising from the shallow 3° flow angle there. Monson (1983) finds that shallow flow angles result both in long oil-flow path lengths which cause a persistence of oil surface waves, and large errors in measured skin friction caused by small errors in applied oil line direction. The gravity correction also becomes large, which makes the theory less accurate. As a result, this angle is probably close to the lower limit for which the present

method can accurately measure the transverse skin-friction component in three-dimensional flows.

3.3 Separated and Reattached Two-Dimensional Flow

Monson, Driver, and Szodruch (1981) applied the laser interferometer method to the measurement of skin friction in the separated and reattached two-dimensional flow behind a rearward-facing step. The tests were performed in a small, high-Reynolds-number, subsonic, continuous-running tunnel. The test-section geometry and test conditions are shown in Fig. 8. The top wall angle is adjustable to alter the free-stream pressure gradient and reattachment length.

Skin-friction measurements were made at several locations in the region of attached flow ahead of the step and throughout the separated and reattached regions downstream of the step. Data were obtained at top wall deflection angles of 0° and 6°. The single-beam method described in Section 2.3 was used because tunnel access limited the laser-beam incidence angle to near-Brewster angles. Pressure-gradient corrections were applied to the data from measured pressure distributions. The corrections were a few percent near reattachment, and negligible elsewhere. The effects of skin-friction gradients were made negligible (to first order) by locating the laser beams on either side of the measurement point as described in Section 2.3.

The measured skin-friction coefficients are shown in Fig. 9 for 0° wall deflection. The data show excellent agreement with Preston tube and "law-of-the-wall" measurements ahead and downstream of the separated region. However, these other methods are not applicable in separated flow. The laser interferometer data show excellent repeatability and self-consistency throughout the separated region, and they are in good qualitative agreement with a theoretical calculation by Sindir (1982). A point of special interest is that by using low-viscosity oil, a repeatable measurement of the very low skin friction of $0.1\ N/m^2$ is obtained where it occurs in the small corner eddy region at the base of the step. This demonstrates

the capability of the method to measure small-scale flow details, as well as very low levels of skin friction, simply by tailoring the oil viscosity to the flow conditions. Also note the ability of the method to successfully measure the mean skin friction close to a reattachment point even though the forces are low and the flow fluctuations are high in that region. This is possible because the oil tends to damp the fluctuations. Similar results were also obtained for a 6° wall-deflection angle.

3.4 Supersonic High-Reynolds-Number Two-Dimensional Boundary Layer Flow

Monson, Driver, and Szodruch (1981) applied the laser interferometer skin-friction method to supersonic high-Reynolds-number flow. The measurements were made in the two-dimensional boundary layer on the nozzle wall of the NASA Ames High-Reynolds-Number Channel I, a variable-temperature blowdown facility designed for stagnation pressures up to 30 atm. Rectangular M_∞ = 2 and 3 nozzles were used. Tunnel optical access required the use of the single-beam method. A thermocouple measured the tunnel-wall temperature changes during the runs and the skin-friction data were corrected for variable oil temperature.

The skin-friction data are shown in Fig. 10 for M_∞ = 2 and 3 over a range of Reynolds number which was changed by varying tunnel stagnation pressure. Oil viscosities were 1000 or 3000 cs, depending on the pressure. The data are compared with the predictions of a reliable, turbulent boundary-layer code. These data agree with the computations within ±10% at both Mach numbers over the Reynolds number range tested.

Although this agreement demonstrates the utility of the laser interferometer method in supersonic high-Reynolds-number flow, the accuracy of the results is less than that achieved in the previously discussed low-speed tests. The reduced accuracy is a consequence of the high skin-friction levels encountered and not the fact that the flow was supersonic. High skin-friction levels produce surface waves on

the oil that persist until the oil is very thin. Thus, few useful fringes can be recorded within the test time available or before the oil becomes too thin to allow a successful measurement. This may represent a fundamental limitation on the laser interferometer method although measurements closer than 5 mm to the oil leading edge, or use of higher viscosity oil, might extend this limit somewhat. In spite of the limitations at high skin-friction levels, the preceding method successfully measured skin-friction levels up to 120 N/m^2; i.e., 40 times higher than the levels of the previously discussed low-speed tests.

3.5 Supersonic Three-Dimensional Delta Wing Flow

Monson, Driver, and Szodruch (1981) measured skin-friction using the laser interferometer method in the three-dimensional vortical flow on the lee side of a delta wing at angle of attack. This is a severe test of the preceding method because of the complex flow over the wing. The general features of the flow are shown in Fig. 11. Typically, this flow is characterized by a primary vortex separation at the leading edge, a reattachment further inboard, and a secondary vortex separation within the primary vortex. Strong surface cross-flow exists between the primary attachment line and the secondary separation line. Consequently, the skin friction can be expected to vary significantly across the span.

Tests on the delta wing were run at $M_\infty = 2$ and 3, and at angles of attack of 0° and 8° in the previously described High-Reynolds-Number Channel I. Axial skin-friction components were measured across the span using the single-beam and three-dimensional methods described in Section 2.3. Variable oil-temperature corrections were included in the data reduction.

Skin-friction data for $M_\infty = 3$ and $\alpha = 8°$ are shown in Fig. 12. The axial skin friction decreases from the centerline outward and then reaches a narrow peak near the primary vortex centerline. It then immediately falls to a very low value near the adjacent separation line and rises to a new but lower peak value under the

secondary vortex. Measurements with other methods for comparison were not possible in this complex flow, nor were theoretical computations available. Thus the accuracy of the laser interferometer data cannot be assessed. However, one might expect a turbulent flat-plate boundary-layer calculation using local-edge conditions to give at least an approximate estimate for skin friction on the centerline of the delta wing. The result of such a calculation is shown in Fig. 12, and the data are observed to be in good agreement with it near the centerline. But, as expected, the calculation fails further outboard where the vortex structures dominate the flow field. Similar results were obtained for other Mach numbers and angles of attack.

Although the accuracy of the above results cannot be fully verified, the good repeatability and agreement with theory on the centerline demonstrate the utility of the laser interferometer method to measure skin friction in very complex flows where other methods are not applicable.

4. Conclusions

A nonintrusive laser interferometer method for measuring skin friction by monitoring the thickness of a thin oil film has been described. The method applies to flows with arbitrarily large pressure gradients and skin-friction gradients, and to three-dimensional flows with unknown direction. The accuracy of this method has been verified in a series of tests incorporating the above effects. These include simple two-dimensional flows, three-dimensional swirling flows, separated flows, supersonic high-Reynolds-number flows, and complex three-dimensional delta-wing flows. Limitations to the method occur in flows possessing high dust levels, at very high skin-friction levels, or when measuring transverse skin-friction components in three-dimensional flows nearly perpendicular to the local flow direction. In spite of these limitations, this method has been used to successfully measure skin-friction levels between 0.1 and 120 N/m^2, and transverse components in three-dimensional flows within 3° of perpendicular to the local flow direction. These results

establish the utility of this method for measuring skin friction in a wide variety of flows where other techniques are limited or impractical.

References

Higuchi, H.; Peake, D.: 1978, Bi-directional, buried-wire skin-friction gauge, NASA TM 78531.

Higuchi, H.; Rubesin, M.: 1981, An experimental and computational investigation of the transport of Reynold's stress in an axisymmetric swirling boundary layer, AIAA paper 81-0416, 19th Aerospace Sciences Meeting, St. Louis, Missouri.

Kline, S.; McClintock, F.: 1953, Describing uncertainties in single-sample experiments, Mech. Engin., vol. 75, no. 1, pp. 3-8.

McAllister, J.; Pierce, F.; Tennant, M.: 1982, Direct Force wall shear measurements in pressure-driven three-dimensional turbulent boundary layers, ASME Journal of Fluids Engineering, vol. 104, no. 2, pp. 150-155.

Monson, D.: 1983, A laser interferometer for measuring skin friction in three-dimensional flows, paper to be presented at the AIAA 21st Aerospace Sciences Meeting, Reno, Nevada.

Monson, D.; Driver, D.; Szodruch, J.: 1981, Application of a laser interferometer skin-friction meter in complex flows, in ICIASF '81 Record, IEEE Publ. 81CH1712-9, Dayton, OH, pp. 232-243.

Monson, D., Higuchi, H.: 1981, Skin friction measurements by a dual-laser-beam interferometer technique, AIAA Journal, vol. 19, no. 6, pp. 739-744.

Sindir, M.: 1982, Numerical Study of turbulent flows in backward-facing step geometries: comparison of four models of turbulence, Ph.D. thesis, U. of Cal., Davis, Calif.

Tanner, L.: 1977, A skin friction meter, using the viscosity balance principle, suitable for use with flat or curved metal surfaces, Journal Phys. E: Sci. Instr., vol. 10, no. 3, pp. 278-284.

Tanner, L.; Blows, L.: 1976, A study of the motion of oil films on surfaces in air flow, with application to the measurement of skin friction, Jour. Phys. E: Sci. Instr., vol. 9, no. 3, pp. 194-202.

Winter, K.: 1977, An outline of the techniques for the measurement of skin friction in turbulent boundary layers, Prog. in the Aerospace Sciences, vol. 18, no. 1, pp. 1-57, Great Britain, Pergamon Press.

Captions to Figures

Fig. 1 - Geometry and notation for two-beam skin-friction measurements in two-dimensional flows

Fig. 2 - Schematic of the two-beam laser interferometer instrument

Fig. 3 - Typical two-beam interferometer fringe record with notation

Fig. 4 - Geometry and notation for two-beam skin-friction measurements in three-dimensional flows

Fig. 5 - Low-speed wind tunnel with center-body rotating test cylinder

Fig. 6 - Comparison of measured and computed skin friction without spin: $V_\infty = 37$ m/s

Fig. 7 - Comparison of measured and computed skin friction with spin: $V_\infty = w_s = 37$ m/s

Fig. 8 - Rearward-facing step-flow experimental geometry and inlet conditions: $V_\infty = 44$ m/s, $M_\infty = 0.13$, $\delta = 1.9$ cm, $H = 1.3$ cm, $Y_o = 8H$, $R_\theta = 5000$

Fig. 9 - Comparison of measured and computed skin friction over a rearward-facing step with separation: $\alpha = 0°$.

Fig. 10 - Comparison of measured and computed tunnel-wall skin friction at supersonic Mach numbers

Fig. 11 - General features of the supersonic lee flow over a delta wing at angle of attack

Fig. 12 - Comparison of measured and computed skin friction on the lee of a delta wing: $\alpha = 8°$, $M_\infty = 3$, $R_{L,\infty} = 2.0 \times 10^6$.

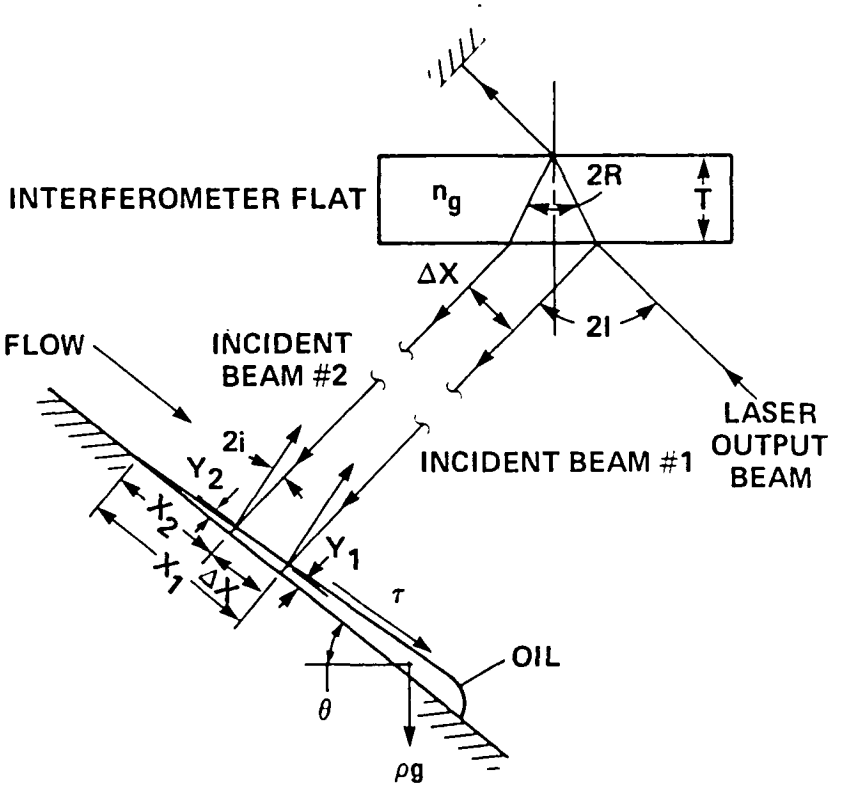
INTERFEROMETER FLAT
n_g
2R
T
ΔX
2I
FLOW
INCIDENT BEAM #2
2i
Y_2
Y_1
INCIDENT BEAM #1
LASER OUTPUT BEAM
L_2
L_1
Δx
τ
OIL
θ
ρg

Fig. 1

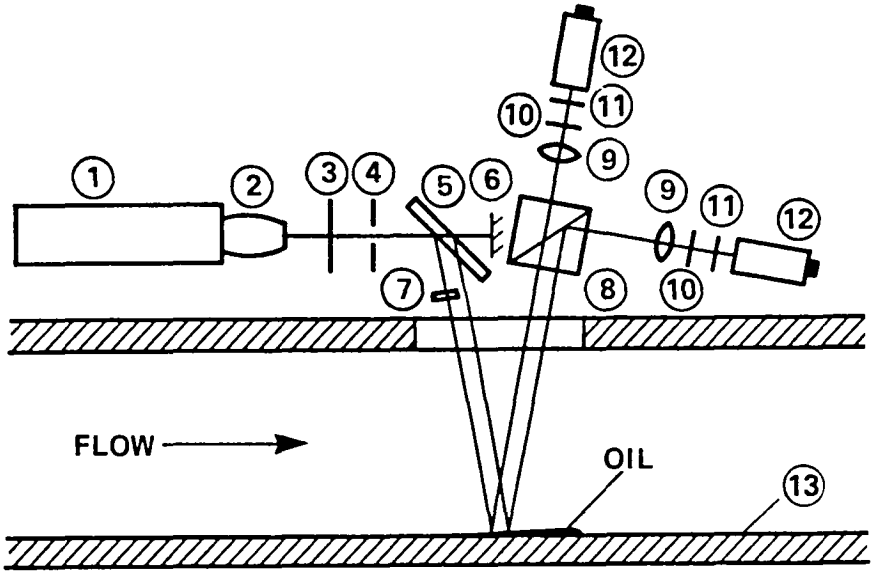

① HE–NE LASER

② TELESCOPE

③ NEUTRAL DENSITY FILTER

④ IRIS DIAPHRAGM

⑤ INTERFEROMETER FLAT

⑥ STOP

⑦ HALF–WAVE RETARDATION PLATE

⑧ POLARIZATION BEAM SPLITTER

⑨ FOCUSING LENS

⑩ POLARIZER

⑪ 6328 Å FILTER

⑫ SILICON PHOTODIODE

⑬ MODEL SURFACE

Fig. 2

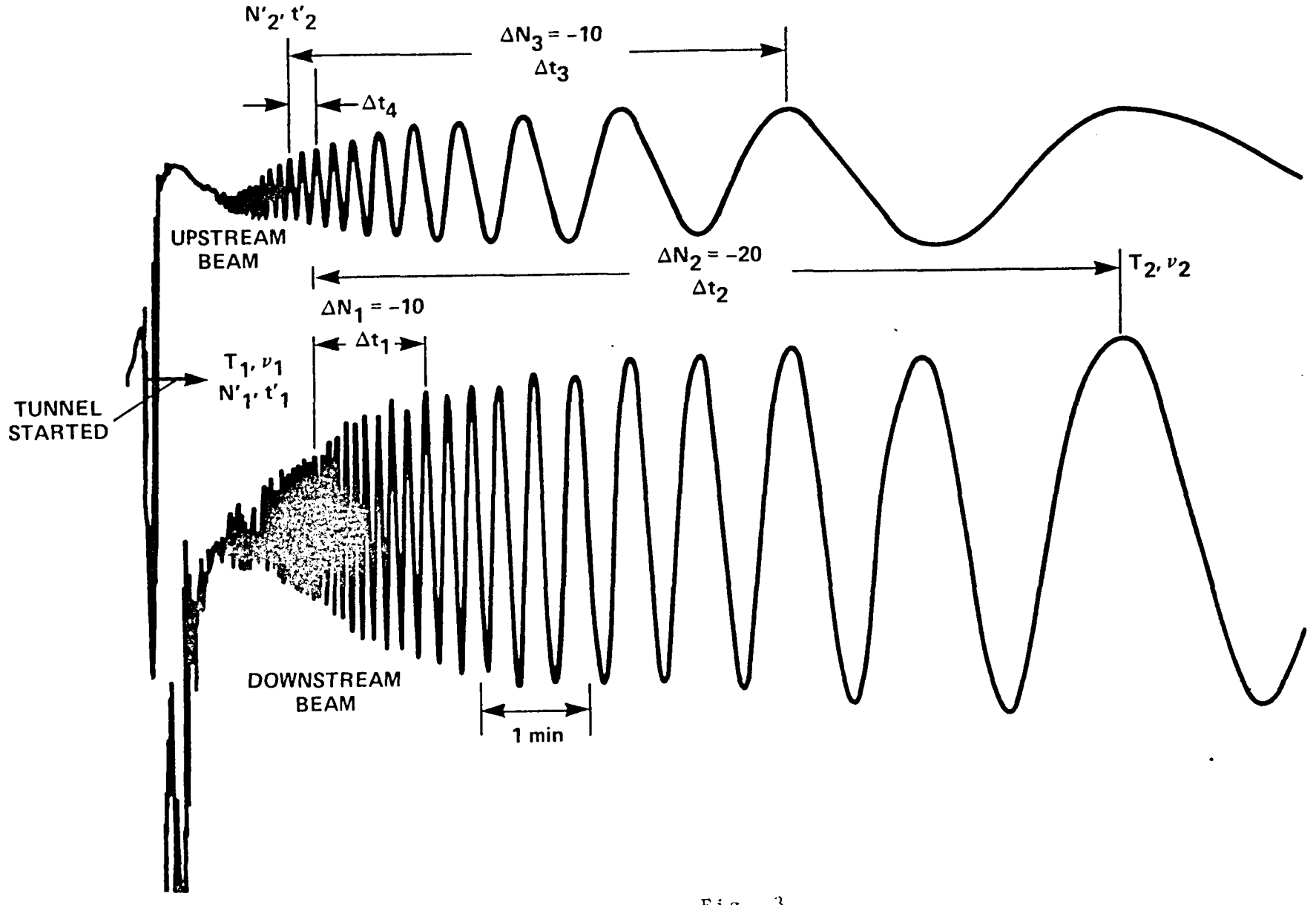
N'2, t'2
ΔN3 = -10
Δt3
Δt4
UPSTREAM
BEAM
ΔN2 = -20
Δt2
T2, ν2
ΔN1 = -10
Δt1
T1, ν1
N'1, t'1
TUNNEL
STARTED
DOWNSTREAM
BEAM
1 min

Fig. 3

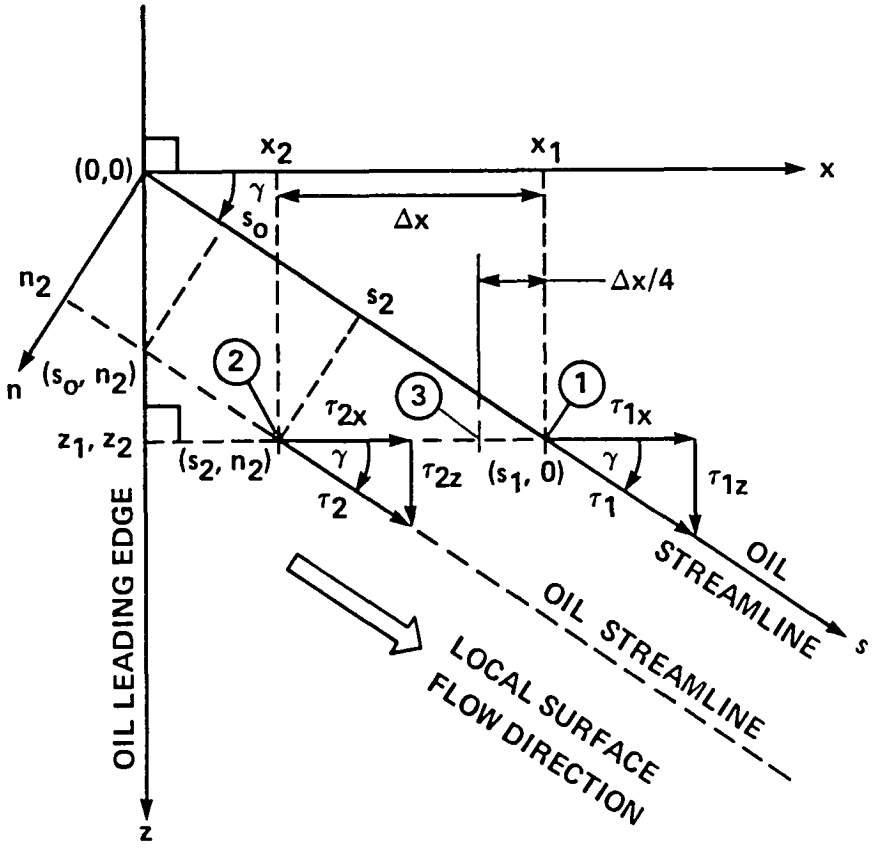
(0,0)
x_2
x_1
x
γ
s_o
Δx
Δx/4
n_2
s_2
n
(s_o, n_2)
2
3
1
τ_{2x}
τ_{1x}
z_1, z_2
(s_2, n_2)
$(s_1, 0)$
τ_{2z}
τ_{1z}
τ_2
τ_1
OIL STREAMLINE
s
OIL STREAMLINE
LOCAL SURFACE FLOW DIRECTION
OIL LEADING EDGE
z

Fig. 4

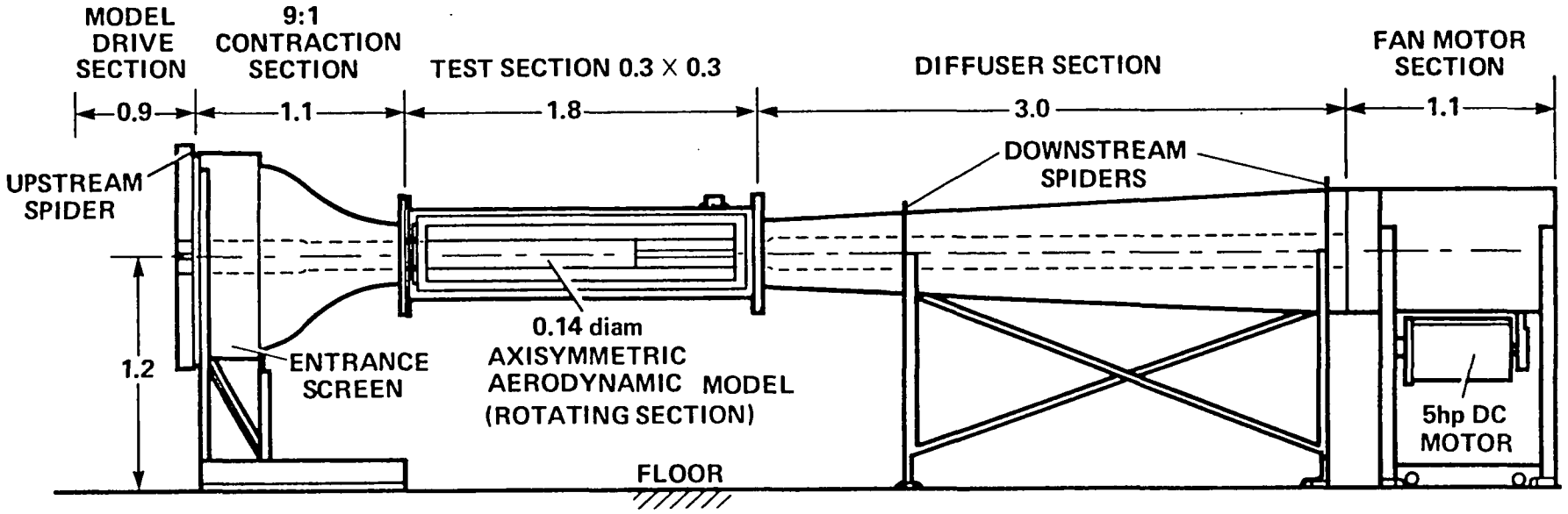
MODEL DRIVE SECTION
9:1 CONTRACTION SECTION
TEST SECTION 0.3 × 0.3
DIFFUSER SECTION
FAN MOTOR SECTION
0.9
1.1
1.8
3.0
1.1
UPSTREAM SPIDER
DOWNSTREAM SPIDERS
1.2
ENTRANCE SCREEN
0.14 diam
AXISYMMETRIC AERODYNAMIC MODEL
(ROTATING SECTION)
5hp DC MOTOR
FLOOR
DIMENSIONS IN m

Fig. 5

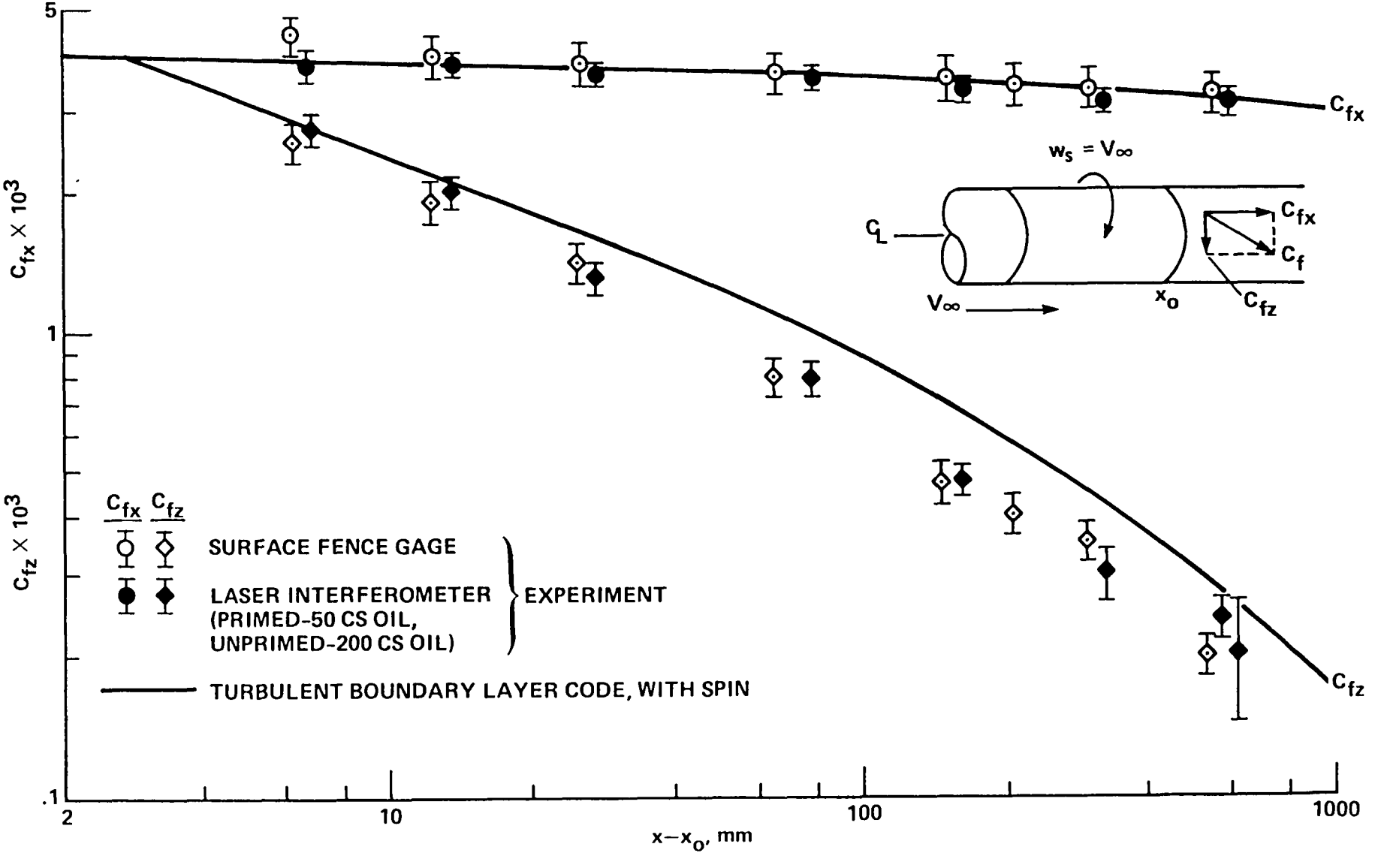
5
1
.1
$C_{fx} \times 10^3$
$C_{fz} \times 10^3$
2
10
100
1000
$x - x_o$, mm
C_{fx}
C_{fz}
$w_s = V_\infty$
C_L
V_∞
x_o
C_f
C_{fx} C_{fz}
SURFACE FENCE GAGE
LASER INTERFEROMETER (PRIMED-50 CS OIL, UNPRIMED-200 CS OIL)
EXPERIMENT
TURBULENT BOUNDARY LAYER CODE, WITH SPIN

Fig. 6

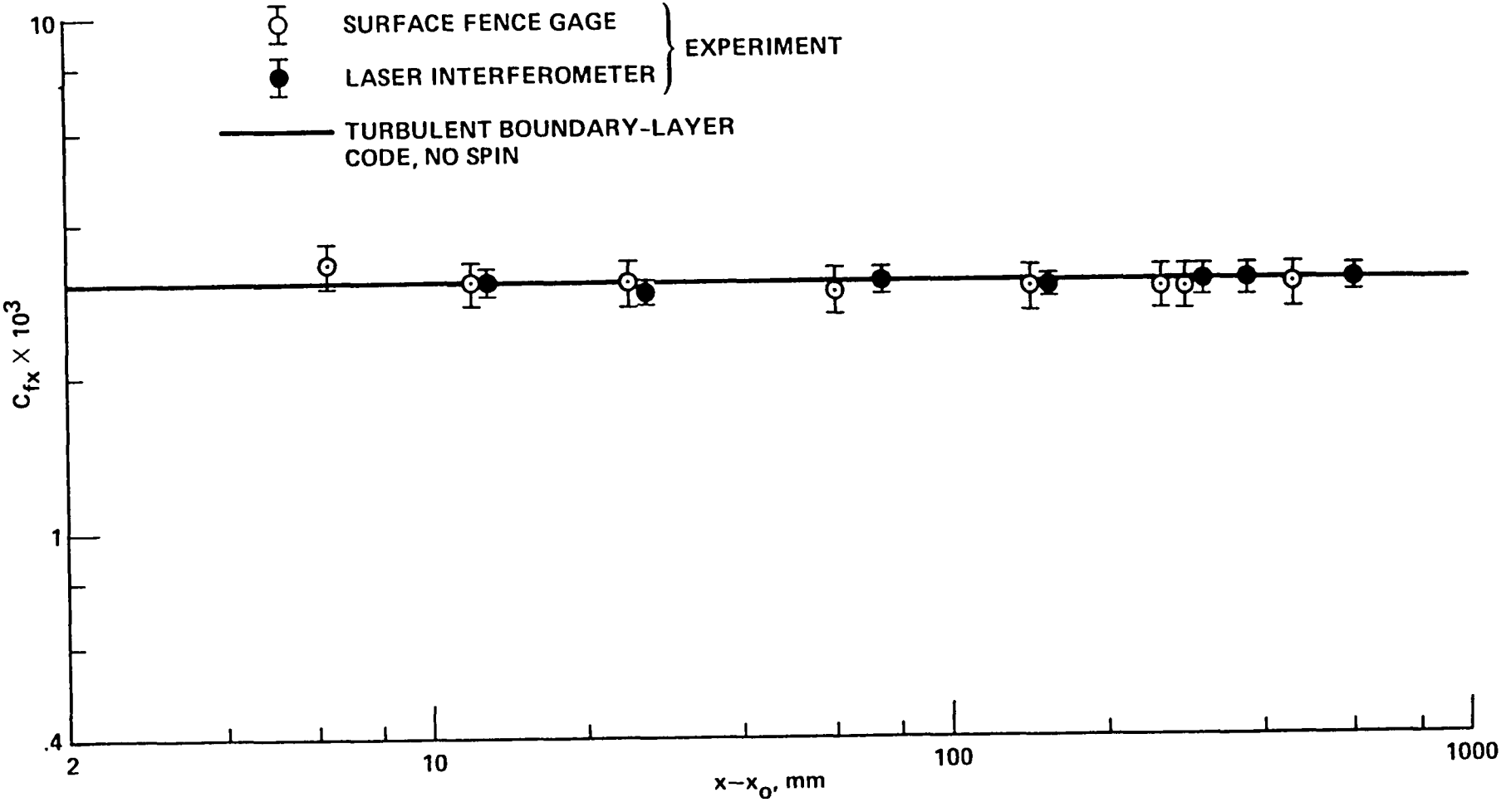
SURFACE FENCE GAGE
LASER INTERFEROMETER
EXPERIMENT
TURBULENT BOUNDARY-LAYER CODE, NO SPIN
10
1
.4
$C_{fx} \times 10^3$
2
10
100
1000
$x-x_o$, mm

Fig. 7

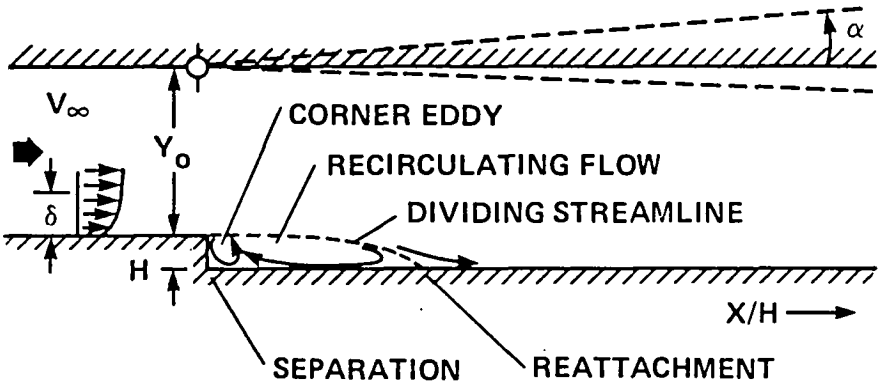
α
V∞
Y₀
δ
H
CORNER EDDY
RECIRCULATING FLOW
DIVIDING STREAMLINE
X/H
SEPARATION
REATTACHMENT

Fig. 8

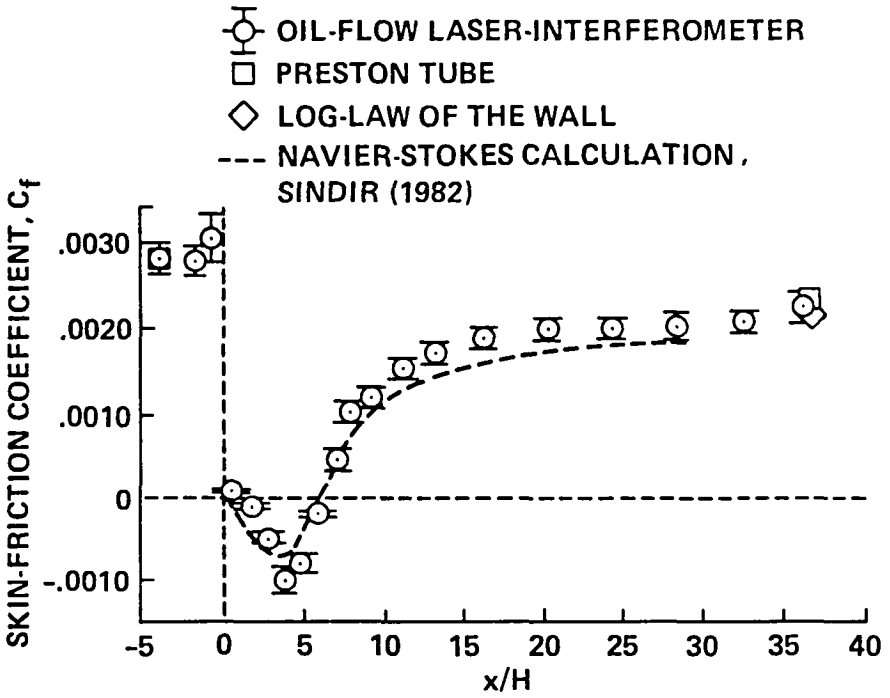
OIL-FLOW LASER-INTERFEROMETER
PRESTON TUBE
LOG-LAW OF THE WALL
NAVIER-STOKES CALCULATION, SINDIR (1982)
SKIN-FRICTION COEFFICIENT, C_f
.0030
.0020
.0010
0
-.0010
-5
0
5
10
15
20
25
30
35
40
x/H

Fig. 9

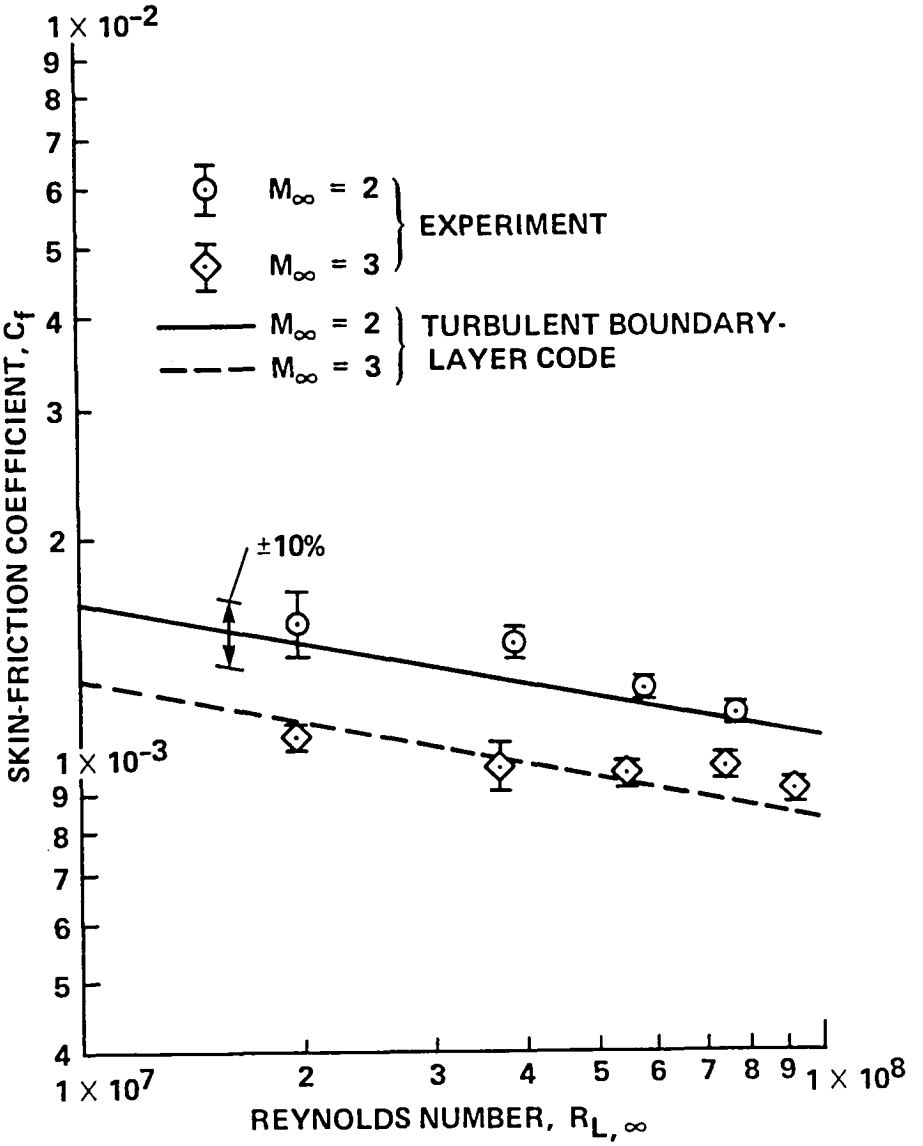
1 × 10⁻²
9
8
7
6
5
4
3
2
1 × 10⁻³
9
8
7
6
5
4
SKIN-FRICTION COEFFICIENT, C_f
M_∞ = 2
M_∞ = 3
EXPERIMENT
M_∞ = 2
M_∞ = 3
TURBULENT BOUNDARY-LAYER CODE
±10%
1 × 10⁷
2
3
4
5
6
7
8
9
1 × 10⁸
REYNOLDS NUMBER, $R_{L,\infty}$

Fig. 10

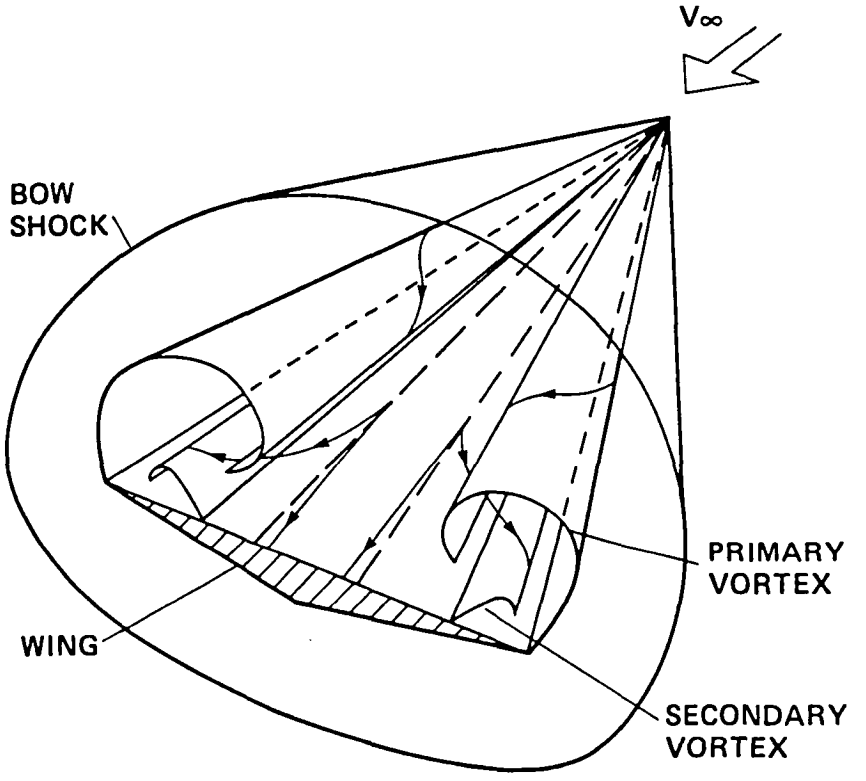

Fig. 11

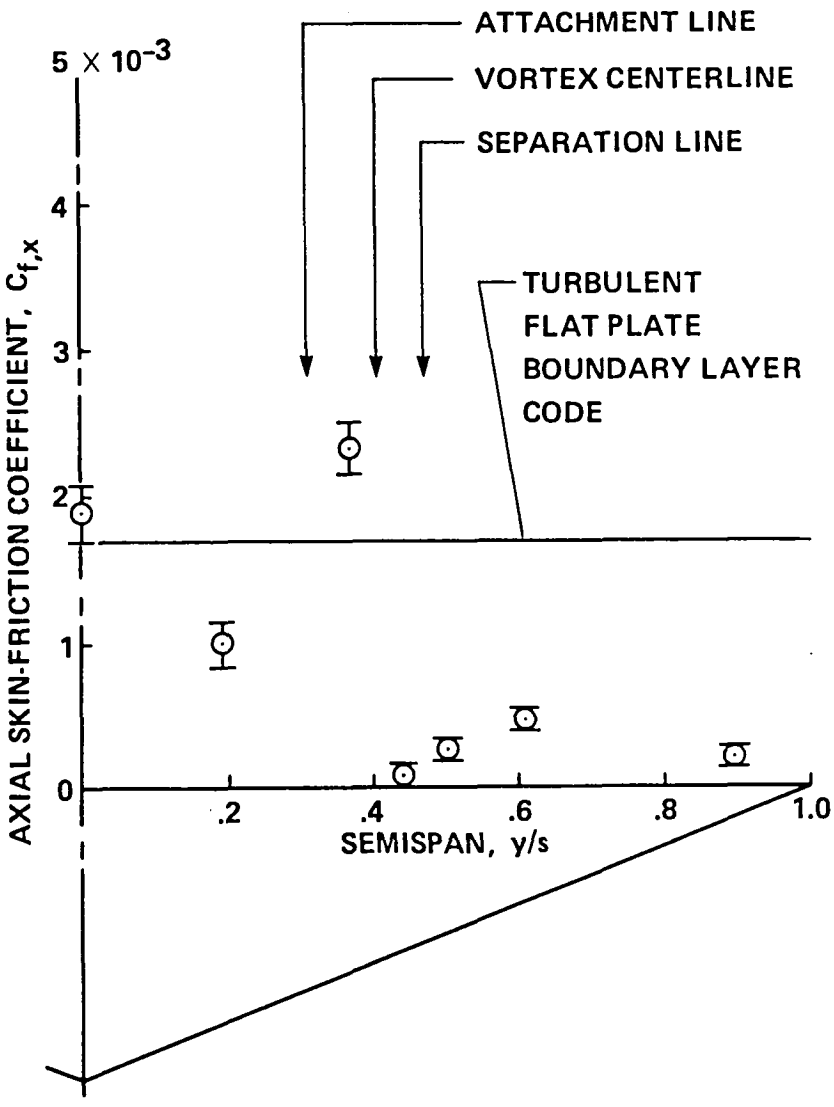
ATTACHMENT LINE
VORTEX CENTERLINE
SEPARATION LINE
TURBULENT
FLAT PLATE
BOUNDARY LAYER
CODE
5 X 10-3
4
3
2
1
0
AXIAL SKIN-FRICTION COEFFICIENT, Cf,x
.2
.4
.6
.8
1.0
SEMISPAN, y/s

Fig. 12

1. Report No.	2. Government Accession No.	3. Recipient's Catalog No.
NASA TM 84300		

4. Title and Subtitle	5. Report Date
A NONINTRUSIVE LASER INTERFEROMETER METHOD FOR MEASUREMENT OF SKIN FRICTION	October 1982
	6. Performing Organization Code
7. Author(s) Daryl J. Monson	8. Performing Organization Report No. A-9077
	10. Work Unit No. T-4234
9. Performing Organization Name and Address NASA Ames Research Center Moffett Field, Calif. 94035	11. Contract or Grant No.
	13. Type of Report and Period Covered Technical Memorandum
12. Sponsoring Agency Name and Address National Aeronautics and Space Administration Washington, D. C. 20546	14. Sponsoring Agency Code 506-51-11-08-00-21

15. Supplementary Notes

Point of Contact: Daryl J. Monson, Ames Research Center, MS 230-3, Moffett Field, California 94035 (415) 965-6193 or FTS 448-6193

16. Abstract

A method is described for monitoring the changing thickness of a thin oil film subject to an aerodynamic shear stress using two focused laser beams. The measurement is then simply analyzed in terms of the surface skin friction of the flow. The analysis includes the effects of arbitrarily large pressure and skin-friction gradients, gravity, and time-varying oil temperature. It may also be applied to three-dimensional flows with unkown direction. Applications are presented for a variety of flows including two-dimensional flows, three-dimensional swirling flows, separated flows, supersonic high Reynolds number flows, and delta-wing vortical flows.

17. Key Words (Suggested by Author(s))	18. Distribution Statement
Fluid mechanics, heat transfer Instrumentation, photography Lasers, Masers	Unlimited Subject Category 35

19. Security Classif. (of this report)	20. Security Classif. (of this page)	21. No. of Pages	22. Price*
Unclassified	Unclassified	36	A02

*For sale by the National Technical Information Service, Springfield, Virginia 22161